Self-energies in BIS and XAS of Al

1992 J. Phys.: Condens. Matter 4 6943

(http://iopscience.iop.org/0953-8984/4/33/008)

J. Phys.: Condens. Matter 4 (1992) 6943–6956. Printed in the UK

Self-energies in BIS and XAS of Al

J J M Michiels, M Grioni† and J C Fuggle‡

Research Institute for Materials, Faculty of Science, University of Nijmegen, Toernooiveld, NL-6525 ED Nijmegen, The Netherlands

Received 2 April 1992

Abstract. The Al K-edge XAS (x-ray absorption spectroscopy) and BIS (Brehmsstrahlung isochromat spectroscopy) spectra are calculated over the energy region $E_F - (E_F + 70$ eV). These spectra are compared with experimental spectra and on the basis of this a discussion of the self-energy corrections is given. The results show that the self-energy corrections, which were obtained by a GW calculation (results are from Horsch and von der Linden), reproduce the experimental peak positions accurately. The same is true for the linewidths above the plasmon energy. To complement the information on linewidths above the plasmon energy with results at lower energies we performed model calculations based on a statistical method. In Al K XAS the core hole effect needs to be included in a calculation of the self-energy corrections, and this is treated on the basis of free electron gas results. There is evidence that the core hole effect and the self-energy corrections cannot be treated independently and additively.

1. Introduction

It has been recognized for over twenty years that a single-particle DOS calculation cannot, strictly speaking, be used to directly predict the spectra of experiments, such as photo-emission (PS), inverse photo-emission or bremsstrahlung isochromat spectroscopy (BIS) and x-ray absorption spectroscopy (XAS). This is because the eigenenergies present in the density of states (DOS) are not excitation energies [1,2]. For systems where the atomic correlations do not dominate completely one can speak of a quasi-particle density of states which represent real excitations of the system and differ from the independent particle DOS by an energy-dependent self-energy. Curiously, although the free-electron systems like Al, Mg and the alkaline metals are amongst the best understood, from a theoretical point of view [3–7] the properties of the self-energies of the unoccupied states relevant to BIS and XAS have been less studied experimentally than in the transition metals, rare earths and compound systems [8–10]. In this paper we undertake such a study, comparing in detail BIS and K XAS spectra with high quality independent-particle DOS calculations. Our aim is to try to quantify the self-energy effects. Unfortunately such comparison is not sensible unless we take account of the transition matrix element variations in both BIS and XAS. We first give a description of the experimental details in section 2, followed by a theoretical section, section 3, in which the simulation of the BIS and XAS spectra is outlined. The results will be presented in section 4 and discussed in section 5.

† Present address: Université de Neuchâtel, Rue A-L Breguet 1, CH-2000 Neuchâtel, Switzerland.
‡ Deceased.

0953-8984/92/336943+14$04.50

Our main conclusions will be that (i) in BIS the plasmon pole model gives a good description of the experimental self-energy corrections, although below the plasmon frequency the model fails because here electron–hole excitations appear to be important and (ii) in K XAS the concept of a system having an extra valence electron and a static core hole potential, for which the self-energy corrections and core hole interaction can be treated independently and additively, is not satisfactory for the case of aluminium.

2. Experimental details

The K XAS spectra of Al were recorded in total photon yield mode using a double crystal monochromotor fitted with quartz single crystals at the BESSY synchrotron. The experimental resolution is of the order of 0.4 eV full width half maximum (FWHM). For both XAS and BIS studies the Al surfaces were prepared by scraping in UHV (approximately 10^{-10} Torr). The BIS spectra, taken from [11], were recorded using an XPS monochromator tuned to the photon energy of the Al Kα line (1486.7 eV) and an electron beam from a cylindrical Pierce gun. Using XPS results the samples were clean (<0.2 monolayers of oxygen) and for long measurements we also checked carefully the region near E_F to ensure that no change with time occurred. The plasmon contribution was subtracted, as described in [11]. For BIS the experimental resolution is of the order of 0.7 eV FWHM Gaussian. An additional 0.2 eV FWHM Lorentzian broadening gives better agreement with the tail of the step at E_F.

3. Theory

In this study we aim to test our ideas on the importance of different contributions to BIS and K XAS spectra. We are especially interested in the self-energy corrections, which relate the LDA DOS to the quasi-particle excitation spectrum. The idea for BIS is the simulation of a BIS spectrum by combining a number of contributions, such as the LDA DOS, the matrix elements for all angular momentum quantum numbers (l = 0, 1, 2, 3) and the self-energy corrections. It must be emphasized that the energy loss of the electron in its high-energy state is not being considered here, because the experimental spectrum has been treated to remove the plasmon losses [11], using the experimentally determined loss function from Al XPS. For Al K XAS a similar procedure will be adopted, now using the p-symmetry projected DOS and matrix elements, but the problem here is how to include the core hole effects. As a starting point we assume that the final state of K XAS is similar to that of BIS, except for the presence of the core hole, and that the self-energy corrections (from BIS) and the core hole effect can be treated independently. To put it in other words: we assume that the quasi-particles in K XAS experience a core hole potential, but the quasi-particle itself and the interaction between the quasi-particles is not changed by this potential. In the following subsections the calculations of bandstructure, transition matrix elements, self-energy corrections and the core hole effect are discussed and the procedure used to combine them is considered.

3.1. The DOS calculations

The DOS was calculated by Zeller [12], using the KKR Green function method [13,14] and the self-consistent potentials of Moruzzi *et al* (Korringa, Kohn and Rostoker) [15,16] for this purpose. The angular momenta are truncated at $l_{max} = 4$. The Brillouin-zone integrations were performed by the tetrahedron integration method [17,18] with 6144 tetrahedrons in the irreducible zone. In these calculations the DOS was calculated up to 68 eV.

3.2. The transition matrix elements

Briefly for BIS we use the formalism of Winter *et al* [19,20] for transition cross sections, which is based on neglecting multiple scattering for the high-energy electron (1.5 keV). This neglect of multiple scattering leads to a localized description of the transition, the so-called 'single-site approximation'. For BIS the overlap integral is calculated between the radial wavefunctions of the incoming electron and the final state at any given energy and angular quantum number l above the Fermi level. The radial wavefunctions are calculated within the muffin-tin potential of Al for a single site, thus making use of the single-site approximation. For K XAS the procedure is very similar, but now the overlap integral is between the radial parts of the 1s wavefunction and the unoccupied p ($l = 1$) states.

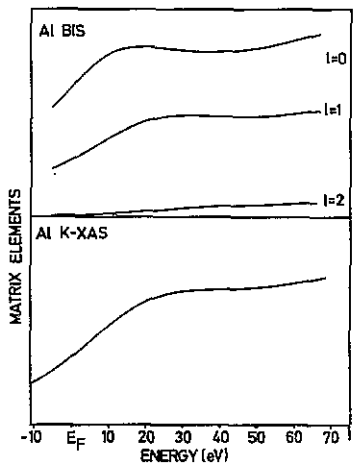

Figure 1. Upper panel: XPS/BIS matrix elements as a function of energy above the Fermi level for different orbital quantum numbers. The matrix elements for $l = 0$, $l = 1$ and $l = 2$ are very large compared with those of higher orbital quantum numbers, so the latter matrix elements are actually too small to be presented on this scale (the intensities are given in arbitrary units). Lower panel: K XAS matrix elements as a function of energy above the Fermi level (the intensities are given in arbitrary units).

The calculated energy dependence of the matrix elements is shown in figure 1 for BIS (upper panel) and K XAS (lower panel). The BIS matrix elements are calculated by Šipr *et al* [21,22]. In the case of BIS the matrix elements depend on the angle between incident electrons and outgoing photons. Although this angle is not usually very well defined, because of the inhomogeneous electric field near the sample, it is still important to consider the angular dependence. Comparison of results from [23],

taking this angular dependence into account, with orientationally averaged matrix elements show that the relative orientation of incident electron and outgoing photons is very important for explaining matrix element effects in, for instance, transition metals. However for aluminium the angular-dependent matrix elements agree very well with the orientationally averaged ones for angles corresponding to the experimental situation.

Returning to figure 1, we see that the important region of these plots is that above the Fermi level and in both cases we note that the matrix elements are increased by a factor of about two between E_F and E_F + 20 eV. Above this energy interval the matrix elements have a nearly constant value. In the case of BIS states of several symmetries contribute to the spectrum but figure 1 shows that only s and p states are important. The matrix elements corresponding to the $l = 0$ states are larger than those for $l = 1$ and are also much larger than those for $l = 2$. Speier *et al* [20] attributed this to the shift in $\langle r \rangle$ to the outer region of the atom, when going to larger l quantum numbers. In these regions the value for the gradient of the muffin-tin potential (the electric field), which slows down the fast electron classically, is smaller and from this it is clear that the potential is more effective for orbitals with lower $\langle r \rangle$, giving rise to larger transition probabilities for lower l.

3.3. Calculated self-energy corrections

In this study we make a comparison between experimental and various theoretical self-energy corrections in order to see the relative importance of electron–hole and plasmon excitations to the excitation spectra. For BIS we use the results from two different methods in treating the self-energy corrections for the unoccupied states in aluminium.

The first one is due to Horsch and von der Linden [24,25]. In their approach the corrections to the quasi-particle energies are calculated self-consistently using the GW approximation, i.e. neglecting vertex corrections in the expansion of the self-energy operator. For the evaluation of the Green function (G) and the screened interaction (W), band structure results are used, so the effect of crystal structure has been taken into account explicitly. The main approximation in Horsch and von der Linden's approach is the generalized plasmon pole model for the dielectric function in W. This approximation can be tested conveniently by comparing simulated and experimental BIS spectra below and above the plasmon energy.

Another method of calculating self-energy corrections, now considering the imaginary part only, is by means of a statistical model, using a model dielectric function [26,27]. For the case of the homogeneous electron gas, the imaginary part of the self-energy correction Δ for an electron with momentum k is given by Quinn [28]:

$$\mathrm{Im}\{\Delta(k)\}_{r_s} = \frac{r_s k_F^2}{2\pi a_0 k} \int_0^{(k^2-k_F^2)/2} \mathrm{d}(\hbar\omega) \int \frac{\mathrm{d}q}{q} \mathrm{Im}\left(\frac{1}{\epsilon_{r_s}(q,\ \omega)}\right)$$

where ϵ is the wavevector (q) and the frequency (ω) dependent dielectric function for the homogeneous electron gas with electron density parameter r_s.

Here

$$r_s(r) = [3/4\pi n(r)]^{1/3} a_0^{-1}$$

and $n(r)$ is the electron density. For a non-homogeneous electron-gas system, such as aluminium, the imaginary part can be approximated by a method developed by

Lindhard and co-workers [29]. In this method the dielectric response of a real system is considered for a small-volume element to be equal to the response of the homogeneous electron gas with the appropriate density and then the imaginary part of the self-energy corrections takes the following form

$$\mathrm{Im}\{\Delta(k)\} = \int \frac{\mathrm{d}^3 r_s}{\Omega} \mathrm{Im}\{\Delta(k)\}_{r_s}$$

where the region of integration is the Wigner–Seitz unit cell of volume Ω. We have evaluated this expression for Al, using the spherically averaged electron density from Ritchie *et al* [26].

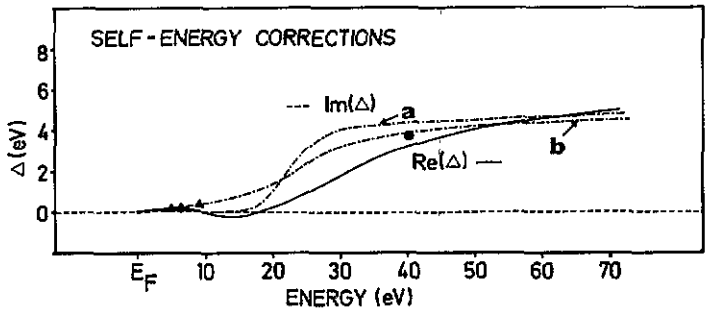

Figure 2. Energy dependence of the real and imaginary parts of the self-energy corrections. The energy on the x-axis is given with respect to the Fermi energy. (*a*) Results of P Horsch and W von der Linden [24], (*b*) statistical model calculations, (*c*) experimental data—●: [30], ▲: [31].

Figure 2 shows the real and imaginary parts of the self-energy corrections. Our results, which are evaluated by means of the statistical method described above, are included in the figure. Considering the real part of the self-energy corrections, we note that this quantity is almost zero up to the plasmon energy, after which it slowly increases. This is normally attributed to the decoupling of the electron from its exchange correlation hole. Turning to the imaginary part of the self-energy corrections Horsch's calculation shows for this quantity a zero value up to the plasmon energy after which it increases rapidly over a range of approximately 5–10 eV and then it increases much more slowly. In this case the increase in $\mathrm{Im}(\Delta)$ and thus the lifetime broadening of the final state results from the creation of plasmons with concomitant loss of energy. This process cannot occur below the plasmon energy and therefore the imaginary part is zero in this energy region. Our approximate treatment of the imaginary part of the self-energy within the statistical model is in good agreement with the results from Horsch and von der Linden for energies above the plasmon frequency. Also these data agree very well with experimental values for electron mean free paths in aluminium [30,31]. Even for energies below the plasmon energy, where the effects of exchange and correlation become important and which are not taken into account completely within the Lindhard dielectric function [32], the results are satisfactory when compared with experimental data. These are also included in figure 2. There are however a few drawbacks connected with this statistical model, such as the lack of self-consistency, and the fact that the Born approximation is not strictly valid for low crystal momenta k.

The real and imaginary parts of the self-energy corrections, which relate the LDA bandstructure to the quasi-particle bandstructure are introduced by means of a convolution [8]:

$$N(E) = \int N_{\mathrm{LDA}}(\epsilon')A(\epsilon',\ E)\ \mathrm{d}\epsilon'$$

where

$$A(\epsilon', E) = (1/\pi)\mathrm{Im}\Delta(\epsilon',\ E)/\{[(E-\epsilon') - \mathrm{Re}\ \Delta(\epsilon',\ E)]^2 + [\mathrm{Im}\ \Delta(\epsilon',\ E)]^2\}.$$

Here N_{LDA} is the LDA DOS. Re $\Delta(\epsilon',\ E)$ and $\mathrm{Im}\Delta(\epsilon',\ E)$ are respectively the real and imaginary parts of the self-energy corrections. It must be emphasized that we did not use the full E-dependence of the corrections in the convolution procedure, because in the experimental spectrum (which is the spectrum we refer to) all intrinsic and extrinsic plasmon losses have already been removed by Hoekstra *et al* [11]. The corrections are introduced by convoluting the DOS with a Lorentzian. The real part of $\Delta(\epsilon',\ E)$ positions the Lorentzian with respect to the E energy zero and the imaginary part of $\Delta(\epsilon',\ E)$ determines the peak width of the Lorentzian. For the case of K XAS an additional contribution to the line broadening is due to the finite lifetime of the core hole. This broadening is 0.42 eV FWHM Lorentzian for Al 1s [2].

3.4. Core hole effect

For a correct description of K XAS spectra it is important to take the creation of the core hole into account. In principle the creation of the core hole is a dynamic perturbation to the system, which should be treated by applying the Fermi golden rule to the many-electron system, including the ground state and excited states N particle wavefunctions. A more simple approach, in which the K XAS spectrum is discussed in terms of a single-particle density of states of the final state, has been used in our study. Here the core hole is treated adiabatically, i.e. the electrons have already relaxed to the presence of the core hole potential. Dynamic effects, such as the MND (Mahan–Nozières–De Dominicis) edge singularity [33–35], are not considered.

In order to obtain the final-state DOS for aluminium, we make use of the results for a free electron gas system. The spirit of the method is to perturb the free electron DOS by an effective core hole potential and apply the changes in the DOS in order to rescale the aluminium DOS. We treat the core hole as a spherically symmetric square well embedded in a zero-potential environment. The Green function for the 'separate' systems is known and the Green function for the composite system can be expressed in terms of these known Green functions [36]. The form the expression takes depends on the spatial coordinates in the Green function. The radii $r_>$ and $r_<$ are both smaller than the muffin-tin radius r_s and $r_< < r_>$.

$$G_l(r_>, r_<, E) = G_{l0}(r_>, r_<, E) + DG^{\mathrm{B}}_{l0}(r_>, r_s, E)G^{\mathrm{B}}_{l0}(r_s, r_<, E)$$

where G^{A}_{l0} and G^{B}_{l0} are the free-electron Green functions of respectively the zero-potential and the square-well region. The l denotes the orbital quantum numbers. For $r_>$ larger and $r_<$ smaller than the muffin-tin radius we have the expression

$$G_l(r_>, r_<, E) = EG^{\mathrm{A}}_{l0}(r_>, r_s, E)G^{\mathrm{B}}_{l0}(r_s, r_<, E)$$

where $r_< < r_s < r_>$. The coefficients D and E are obtained by requiring that the Green functions and their derivatives should be continuous at the square-well radius. From this the total Green function and density of states can be constructed for the composite system. The only free parameter in the effective core hole potential is the square-well depth (the square-well radius is fixed at the value of the muffin-tin radius). This parameter can be found by using the requirement that the total screening charge is unity for ideal metals. The connection between total screening charge and well depth is made by using the Friedel sum rule

$$\Delta Z = \frac{2}{\pi}\sum_{l=0}^{\infty}(2l+1)\delta_l(E_F)$$

in which the phase-shift values are functions of the square-well depth [37]. This method has been extrapolated to the case of aluminium, by replacing the Green function for the zero-potential region by the aluminium Green function. This gives similar expressions for the total Green function of the composite system, though the energy dependence of the coefficients D and E is changed. An approximate way of treating this energy dependence is by scaling the unperturbed Al Green function directly

$$G_l^{\mathrm{Al+well}}(r_>, r_<, E) = \left[N_l^{\mathrm{FEG+well}}(E)/N_l^{\mathrm{FEG}}(E)\right] G_l^{\mathrm{Al}}(r_>, r_<, E).$$

Although the approximation proves to be a good one for the Al DOS, care still has to be taken when interpreting the final result. Replacement of the scaling by some approximate quotient changes the Green function into a function that does not obey the Green function requirements exactly. For nearly free electron systems, such as the simple metals, the approximation is believed to be satisfactory because the screening of the core hole is approximately similar to that in the free electron gas. In the limit of a free electron gas the applied scaling is exact.

4. Results and interpretation

4.1. Al BIS

In the last section we discussed how to construct a spectrum (K XAS or BIS) by combining different contributions, from DOS, matrix elements and self-energy corrections. We illustrated these different steps in figure 3 for the case of BIS.

Figure 3(*a*) contains the total DOS and the experimental Al BIS spectrum. The total DOS has been broadened to account for the experimental resolution, and additionally a Lorentzian of $0.12(E - E_F)$ eV has been taken into account for the lifetime of the excited electron. This latter contribution is purely empirical and will be analysed below in more detail, but some broadening must be applied here to allow any sensible comparison. The major discrepancies between the experimental and 'theoretical' spectra in figure 3(*a*) are the shape between E_F and E_F + 25 eV, with a strong peak in the theory at $\simeq$ 22 eV and shifts of the peak energies, e.g. at $\simeq$ 39 eV (experimental) and $\simeq$ 35 eV (theory) or $\simeq$ 55 eV (experimental) and $\simeq$ 50 eV (theory).

Some of the discrepancies are removed as soon as the matrix elements are included in figure 3(*b*)—for instance the spurious peak at $\simeq$ 22 eV due to the contribution from states of predominantly d symmetry which have a relatively low weight in the spectrum. Also the relative intensity at $\simeq$ 30 eV has decreased, because this is influenced by the large weight of f symmetry in this energy region [11,38] and these too have a low weight in BIS. Summarizing, introduction of the matrix elements leads to a fairly good agreement in spectral shape.

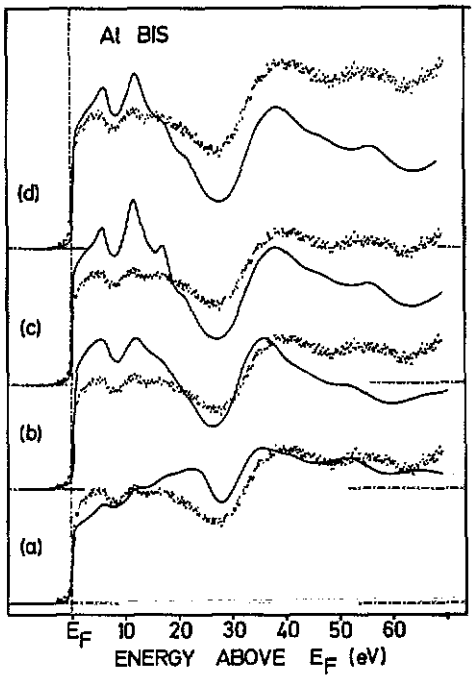

Figure 3. Comparison of experimental BIS spectrum (data points) of Al with the calculated spectra. These calculated spectra are (*a*) the broadened total DOS (Lorentzian broadening of 0.20 eV FWHM and a Gaussian broadening of 0.7 eV FWHM to account for the experimental resolution and an empirical energy-dependent broadening of $0.12(E - E_F)$ eV FWHM, representing the finite lifetime of the extra valence electron, (*b*) the broadened DOS with transition matrix elements included, (*c*) the DOS with matrix elements, and self-energy corrections from Horsch, (*d*) the spectrum from (*c*) but with the line broadening results from the statistical model.

We now consider in detail the effect of the introduction of self-energy corrections (real and imaginary parts), using the Horsch and von der Linden results [24] and our results on the imaginary part of the self-energy (see also figure 2). In figure 3(*c*) Horsch's data are folded into the theoretical spectrum. Beginning with the real part, this clearly results in an improvement of peak positions over the whole energy range. For instance the minimum at $\simeq$ 27 eV and the maximum at $\simeq$ 39 eV are now well aligned. However, the use of Horsch's data for the imaginary part of the self-energy corrections has led to new problems in the region between E_F and $\simeq (E_F + 18$ eV), where the structure in the theoretical curve is much too sharp and strong. This is primarily because Horsch's Im Δ curve gives no broadening up to the plasmon frequency (see figure 2), which is in turn a consequence of the plasmon pole

approximation. To check the influence of the low-energy excitations we applied the results of the statistical model calculations, which are in agreement with experimental data on lifetime broadening in this energy region [31]. The results in figure 3(*d*) show better agreement with less sharp structure in the theoretical spectrum in the region up to E_F + 18 eV.

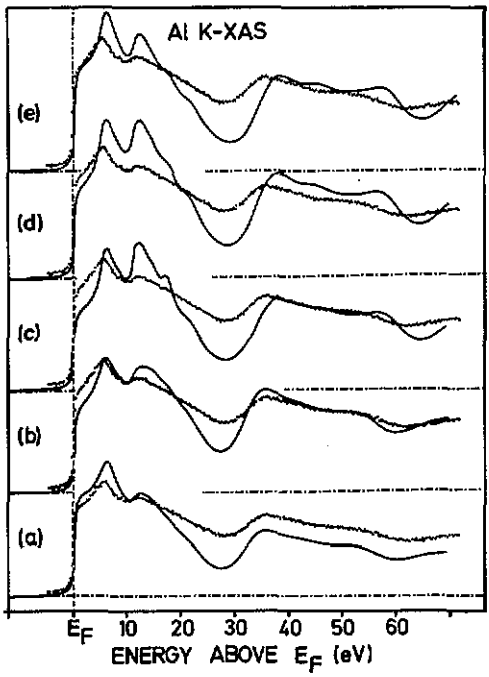

Figure 4. Comparison of experimental K XAS spectrum (data points) of Al with the calculated spectra. These calculated spectra are (*a*) the broadened p DOS (Gaussian broadening of 0.4 eV FWHM to account for the experimental resolution and a Lorentzian broadening of 0.42 eV FWHM due to the core hole lifetime and an empirical energy-dependent broadening of $0.12(E-E_F)$ eV FWHM to account for the finite lifetime of the extra valence electron, (*b*) the broadened p DOS with matrix elements included, (*c*) the p DOS with matrix elements, and self-energy corrections from Horsch, (*d*) the spectrum from (*c*) but with the line broadening from the statistical model, (*e*) the p DOS in which the effect of the completely screened core hole has been taken into account, combined with all the self-energy corrections used in (*d*).

We must now consider the distribution of spectral weight in more detail. The agreement in figure 3(*d*) is not very good, with too little weight above E_F + 20 eV. This is probably because the actual experimental BIS spectrum has been obtained by subtracting the plasmon losses. A small change in the plasmon weight does not lead to peak shifts or changes, but it can influence the 'slope' of the spectrum. In view of this uncertainty it is not sensible to speculate further on the spectral weight discrepancy for BIS.

4.2. Al K XAS

Figure 4(*a*) contains the p DOS and the experimental K XAS spectrum. The p DOS has been broadened to account for the experimental resolution and additionally the broadening due to the core hole (0.42 eV FWHM Lorentzian) and the finite lifetime of

the extra valence electron have been taken into account ($0.12(E-E_F)$ eV). The latter contribution is empirical, but it is necessary in order to make a sensible comparison of the p DOS with the experimental spectrum possible. The p DOS has much less weight in the region around 23 eV and at higher energies. In the total DOS much of this weight comes from the Al d and f states. The main structure of the Al K XAS and p DOS curves is very similar and the agreement of peak and valley positions is rather good, and actually better than the corresponding curves for BIS in figure 3(*a*). This point will be discussed further below. We note that above E_F + 18 eV the theoretical spectrum has too little weight.

In figure 4(*b*) the matrix elements have been included and consequently the intensity distribution is better reproduced. However, a number of serious discrepancies remain, such as the lack of spectral weight just above the Fermi level and the excess spectral intensity in the energy region (E_F + 11 eV)–(E_F + 19 eV). Also the gap-like feature at 27 eV is far too low. These discrepancies cannot be explained by failures of the matrix element calculations, because the matrix elements vary slowly with energy, and small errors do not lead to disagreement between theoretical and experimental spectra in relatively small-energy regions. We return to these points in the discussion in section 5. Figure 4(*c*) contains the theoretical K XAS spectrum, in which Horsch and von der Linden's real and imaginary parts of the self-energy corrections have been introduced. The corrections do not lead to any improvement: the theoretical peak positions for peaks above E_F + 25 eV agree less well with experiment and the theoretical linewidth below E_F + 25 eV is clearly too small. Moreover, the discrepancies discussed in connection with figure 4(*b*) are still present in figure 4(*c*).

Some of the discrepancies are removed when we introduce Im Δ from our statistical model calculation into figure 4(*d*), in the same way as for BIS. For instance the intensity ratio of the peaks near E_F (at E_F + 6 eV and E_F + 12 eV) has improved over that in figure 4(*c*). Also the linewidth below E_F + 25 eV and the depth of the gap-like feature at E_F + 27 eV is now in better agreement with experiment.

However the problems of spectral weight near E_F (E_F–(E_F + 20 eV)), the depth of the minimum near 27 eV, and the discrepancy in the energy of the peaks above $\simeq$ 30 eV all remain. In figure 4(*e*) the model discussed in section 3.4 has been used to include the effect of the core hole potential. The application of the model shifts weight to the Fermi level, and as a result shifts the peak at approximately E_F + 6 eV and E_F + 12 eV to slightly lower energies. These changes are consistent with our experience of the influence of core holes within the Clogston–Wolff model [39–42] and also with *ab initio* impurity calculations [9, 43, 44]. At higher energies the influence of the core hole on the distribution of spectral weight is negligible. Summarizing, the changes result in better agreement with experiment up to about 15 eV above the Fermi level. We are, however, left with serious problems at higher energies, where the theory overestimates the depth of the minimum near E_F + 27 eV and the peaks at approximately E_F + 38 eV and E_F + 56 eV in the theoretical spectrum are clearly at too high energy. Such discrepancies are large and we must wonder about the significance of the good agreement between E_F and E_F + 15 eV.

5. Discussion

5.1. Al BIS

In section 4.1 we compared the experimental BIS spectrum after plasmon subtraction

with theoretical simulations incorporating a high quality KKR single-particle calculation, transition matrix elements and various empirical and theoretical models for obtaining the real and imaginary parts of the self-energy corrections. The interpretation of these data leads us to the conclusion that below the plasmon frequency electron–hole excitations are important for an explanation of the lifetime broadening and these excitations are not included in the generalized plasmon pole model of Horsch and von der Linden.

The transition matrix elements were seen to be important to reproduce the correct form of the spectrum, whereby the major effect is simply that the BIS cross sections decrease with orbital quantum number of the electron in the final state. The peak positions are only reproduced in an acceptable way if we take into account the real part of the self-energy corrections, which is dominated by the 'decoupling' of the electron from its exchange correlation hole. For Al, Horsch's treatment of the real part of the self-energy corrections, using a plasmon pole approximation, seems to be perfectly adequate for this task. By contrast, the plasmon pole approximation leads to discrepancies between theoretical and experimental 'peakwidths', particularly up to $\simeq 23$ eV above E_F. We are fairly confident in attributing this discrepancy to the effect of other excitations, whereby the electron–hole pair creation is probably the most important, as was established by model calculations. Another important point, which has not been discussed yet, is the energy range in which the quasi-particle concept is valid and in which we can treat the many-body interactions as a sort of correction to the LDA DOS. From results on the single-particle spectrum of the degenerate electron gas by Lundqvist [45], it is clear that the quasi-particle peak in the spectral function for this system is of considerable weight. When we extrapolate the results for the uniform electron gas with appropriate electron density to the case of the non-homogeneous electron gas of aluminium, we expect the quasi-particle picture to be valid for all relevant energies above E_F.

5.2. Al K XAS

It was shown in section 3 that the theoretical K XAS spectrum can be constructed from various contributions, such as the p DOS, the matrix elements, the BIS self-energy corrections, the core hole lifetime and the core hole potential. In our case the relative success in simulating the BIS spectrum indicates that the treatments to calculate the DOS, the transition matrix elements and the real part of the self-energy corrections were all quite adequate. It is true that the plasmon pole approximation appeared to be inadequate for reproduction of the imaginary part of Δ, but we were able to calculate this quantity in a satisfactory way by using a statistical model.

However, the procedure didn't lead to a very good agreement between theoretical and experimental spectra for K XAS and we want to concentrate on two unsatisfactory features of the theoretical spectrum, which appear in a comparison with the experimental spectrum (figure 4(*e*)). First we note that in a narrow energy range around 27 eV the relative theoretical intensity drops to about half of that actually observed, before recovering at higher energies. The matrix elements vary rather slowly with energy and we see no possibility to introduce any correction to these matrix elements in order to remove the discrepancy. One can always try to fill up the minimum by increasing the lifetime broadening to the lower and higher energy side of the minimum, but this is equivalent to introducing a very complicated variation of the imaginary part of the self-energy corrections. One can also fill up the minimum with a complicated energy dependence of the real part of the self-energy correction in

order to compress and stretch the spectral weight. Again this should not be done without a good physical justification.

The second discrepancy we pinpoint is in the energy of the experimental (theoretical) 'peaks' at 36 (39) eV and 53 (58) eV in the theoretical and experimental K XAS spectra of figure 4(*e*). Introduction of the core hole potential does not lead to any improvement of agreement concerning these peak positions. Considering these discrepancies we conclude that the procedure of treating the core hole effect and BIS self-energy corrections independently is probably an oversimplification. Apparently the core hole effect is important in determining the properties of the quasi-particles in K XAS, such as the excitation energies.

In this study the final-state rule [46,47] has been applied for calculating the K XAS spectra, which is a good approximation in most of the one-electron treatments of x-ray absorption in metals. However, for a complete description of the spectra, dynamical effects at the Fermi edge have to be taken into account, as shown by Neddermeyer [48] for edge singurities in x-ray emission and absorption spectra of magnesium and aluminium. Another dynamical effect, which has been treated theoretically by Bose and Longe [49] is plasmon excitation. We do not observe a clear plasmon structure in our K XAS spectra of aluminium, though there are K XAS experiments of aluminium, performed with long accumulation periods, that show very weak structures at the theoretically predicted energy positions [50]. Care has to be taken however, to distinguish between sharp features in the band structure and plasmon excitations, which might be important for aluminium.

6. Summary and conclusions

In this paper we have made a comparison between the experimental and theoretical BIS and K XAS spectra of aluminium up to about $\simeq 70$ eV above threshold in order to quantify the self-energy corrections for each technique. The individual components of the calculations were relatively 'state of the art'. We come to the following conclusions:

(i) In order to reproduce correctly the peak positions in BIS it is necessary to take into account the real part of the self-energy corrections, which produces shifts up to about 10%.

(ii) In order to reproduce a BIS spectrum it is necessary to introduce an energy dependent broadening of the DOS. This is equivalent to the lifetime broadening associated with the excited extra valence electron in the final state and rises to about 5 eV (FWHM) at about 50 eV. At higher energies, i.e. approximately more than 20 eV above E_F, Horsch's calculations of the imaginary part of Δ appear adequate to this task, but below this energy an extra energy-dependent broadening must be included, and it is clear that the plasmon pole approximation is not adequate.

(iii) The energy-dependent broadening, which has been calculated by means of a statistical model, is in good agreement with the experimentally determined lifetime broadening in BIS.

(iv) In K XAS the core hole effect and the (BIS) self-energy corrections cannot be included in an 'additive' way in the LDA spectrum, in order to reproduce a correct K XAS spectrum. A more satisfactory treatment of the self-energy corrections in K XAS needs integration of both treatments.

Acknowledgments

This paper is dedicated to the memory of John Fuggle, who died in December 1991 and didn't see the paper completed. We are grateful for stimulating discussions and correspondence with L Hedin, J E Inglesfield, P Horsch, J F van Acker, R Zeller, W Speier, O Šipr and others. This work has been supported in part by the Stichting voor Fundamenteel Onderzoek der Materie (FOM) with financial support from the Nederlandse Stichting voor Wetenschappelijk Onderzoek (NWO), the Netherlands.

References

[1] Hedin L and Lundqvist S 1969 *Solid State Physics* vol 23 (New York: Academic) p 1
[2] Fuggle J C and Inglesfield J E (ed) 1991 *Unoccupied Electronic States* (Berlin: Springer)
[3] Lässer R and Fuggle J C 1980 *Phys. Rev.* B **22** 2637
[4] Jensen E and Plummer E W 1985 *Phys. Rev. Lett.* **55** 1918
[5] Kortboyer S W, Grioni M, Speier W, Zeller R, Watson L M, Gibson M T, Schäfers F and Fuggle J C 1989 *J. Phys.: Condens. Matter* **1** 5981–7
[6] Plummer E W 1985 *Surf. Sci.* **152/153** 162–79
[7] Levinson H J, Greuter F and Plummer E W 1983 *Phys. Rev.* B **27** 727
[8] Jackson W B and Allen J W 1988 *Phys. Rev.* B **37** 4618
[9] Weijs P J W, Czyzyk M T, van Acker J F, Speier W, Goedkoop J B, Hendrix H J M, de Groot R A, van der Laan G, Buschow K H J, Wiech G and Fuggle J C 1990 *Phys. Rev.* B **41** 11899
[10] Speier W, Zeller R and Fuggle J C 1985 *Phys. Rev.* B **32** 3597
[11] Hoekstra J H W M, Speier W, Zeller R and Fuggle J C 1986 *Phys. Rev.* B **34** 5177
[12] Zeller R private communications
[13] Korringa J 1974 *Physica* **13** 392
[14] Kohn W and Rostoker N 1954 *Phys. Rev.* **94** 1111
[15] Moruzzi V L, Jancik J F and Williams A R 1978 *Calculated Electronic Properties of Metals* (New York: Pergamon)
[16] Moruzzi V L, Jancik J F and Williams A R 1977 *Phys. Rev.* B **15** 2584
[17] Lehmann G and Taut M 1972 *Phys. Status Solidi* b **54** 469
[18] Jepsen O and Andersen O K 1971 *Solid State Commun.* **9** 1763
[19] Winter H, Durham P J and Stocks G M 1984 *J. Phys. F: Met. Phys.* **14** 1047
[20] Speier W, Fuggle J C, Durham P J, Zeller R, Blake R J and Sterne P 1988 *J. Phys. C: Solid State Phys.* **21** 2621
[21] Vackař J, Šimůnek A and Šipr O 1989 *Phys. Rev. Lett.* **63** 2076
[22] Vackař J, Šimůnek A and Šipr O 1991 *Comput. Phys. Commun.* **66** 259–65
[23] Šipr O private communication
[24] Horsch P private communication
[25] von der Linden W and Horsch P 1988 *Phys. Rev.* B **37** 8351
[26] Tung C J, Ashley J C and Ritchie R H 1979 *Surf. Sci.* **81** 427–39
[27] Penn D R 1987 *Phys. Rev.* B **35** 482
[28] Quinn J J 1962 *Phys. Rev.* **126** 1453
[29] Lindhard J and Schraff M 1953 *K. Danske Vidensk. Selsk. Mat.-Fys. Meddr.* **27** 15
Lindhard J, Schraff M and Schiott H E 1963 *K. Danske Vidensk. Selsk. Mat.-Fys. Meddr.* **33** 14
[30] Tracy J C 1974 *J. Vac. Sci. Technol.* **11** 280
[31] Callcot T A and Arakawa E T 1975 *Phys. Rev.* B **11** 2750
[32] Penn D R 1976 *Phys. Rev.* B **13** 5248
[33] Mahan G D 1967 *Phys. Rev.* **163** 612
[34] Anderson P W 1967 *Phys. Rev. Lett.* **18** 1049
[35] Nozières P and De Dominicis C T 1969 *Phys. Rev.* **178** 1097
[36] Inglesfield J E 1972 *J. Phys. F: Met. Phys.* **2** 63
[37] Merzbacher E 1961 *Quantum Mechanics* 2nd edn (New York: Wiley)
[38] Hoekstra H J W M, Fuggle J C, Speier W and Sarma D D 1987 *J. Electron. Spectrosc. Relat. Phenom.* **42** 27–39
[39] Wolff P A 1961 *Phys. Rev.* **124** 1030

[40] Clogston A M 1962 *Phys. Rev.* **125** 439
[41] Speier W, van Acker J F and Zeller R 1990 *Phys. Rev.* B **41** 2753
[42] van Acker J F, Speier W and Zeller R 1991 *Phys. Rev.* B **43** 9558
[43] Zeller R 1988 *Z. Phys.* B **72** 79–85
[44] Braspenning P J, Zeller R, Lodder A and Dederichs P H 1984 *Phys. Rev.* B **29** 703
[45] Lundqvist B I 1967 *Phys. Kondens. Mater.* **6** 193
[46] Mahan G D 1980 *Phys. Rev.* B **21** 1421
[47] Davis L C and Feldkamp L A 1981 *Phys. Rev.* B **23** 4269
[48] Neddermeyer H 1976 *Phys. Rev.* B **13** 2411
[49] Bose S M and Longe P 1978 *Phys. Rev.* B **18** 3921
[50] Sénémaud C 1978 *Phys. Rev.* B **18** 3929